

A procedure for the evaluation of flow stress of sheet metal by hydraulic bulge test using elliptical dies

Lucian LĂZĂRESCU^{1,a}, Ioan Pavel NICODIM^{1,b}, Dan-Sorin COMȘA^{1,c}
and Dorel BANABIC^{1,d}

¹CERTETA Research Centre, Technical University of Cluj-Napoca, Cluj-Napoca Romania

^alucian.lazarescu@tcm.utcluj.ro, ^bioan.nicodim@tcm.utcluj.ro, ^cdscomsa@tcm.utcluj.ro,
^dbanabic@tcm.utcluj.ro

Keywords: Analytical Approach, Elliptical Die, Flow Stress, Hydraulic Bulge Test.

Abstract. The paper describes a new experimental procedure for the determination of the curves relating the equivalent stress and equivalent strain of sheet metals by means of the hydraulic bulge tests through elliptical dies. The procedure is based on an analytical model of the bulging process and involves the measurement of only two parameters (pressure acting on the surface of the specimen and polar deflection).

Introduction

The hydraulic bulge test through elliptical dies is used for obtaining different load paths in the polar region of the specimen. The adjustment of the load path is achieved by modifying the ellipticity of the die. There are only few papers dealing with the determination of the hardening curves in the more general case of the bulge tests with non-circular dies. Yousif [1] investigated the geometry of the deformed specimen and the fracture mode of the sheet metals subjected to bulging with elliptical dies. He obtained stress-strain curves and forming limit diagrams for brass, copper and mild steel. Banabic [2] developed analytical models for the computation of the pressure-time relationship for the bulging through elliptical dies of both strain hardening and superplastic materials. Ragab [3] determined experimental curves relating the equivalent stress and the equivalent strain of sheets using dies with circular, rectangular and elliptical apertures. Rees [4] presented a theoretical analysis of the polar deformation during the bulging through elliptical dies. He validated the model by experiments that were focused on examining the equivalence between the polar flow in the case of the bulge test and the plastic flow in uniaxial tension. The authors of this paper previously developed a methodology for a more accurate determination of the hardening curves in the case of the bulge test through circular dies [5, 6]. Their experimental procedure is based on an improved version of Kruglov's formula [7] used for evaluating the current values of the polar thickness.

This paper presents an experimental methodology for the determination of the hardening curves by means of the hydraulic bulge tests through elliptical dies. The procedure is based on an analytical model of the bulging process and involves the measurement of only two parameters (pressure acting on the surface of the specimen and polar deflection).

Analytical model of the bulging process

In the case of the bulge test, a disc shaped specimen is firmly clamped under a ring at the top of a hydraulic cylinder. The specimen is then deformed by a uniformly increasing pressure applied on its bottom face. Throughout this study, the free surface of the specimen is schematized as shown in Figure 1. More specific, the deformed region is approximated by a rotational ellipsoid (the rotational axis is horizontal in Figure 1). As a consequence, the profile of the deformed specimen is assumed to be elliptic along the major axis (b) and circular along the minor axis (a) of the die hole.

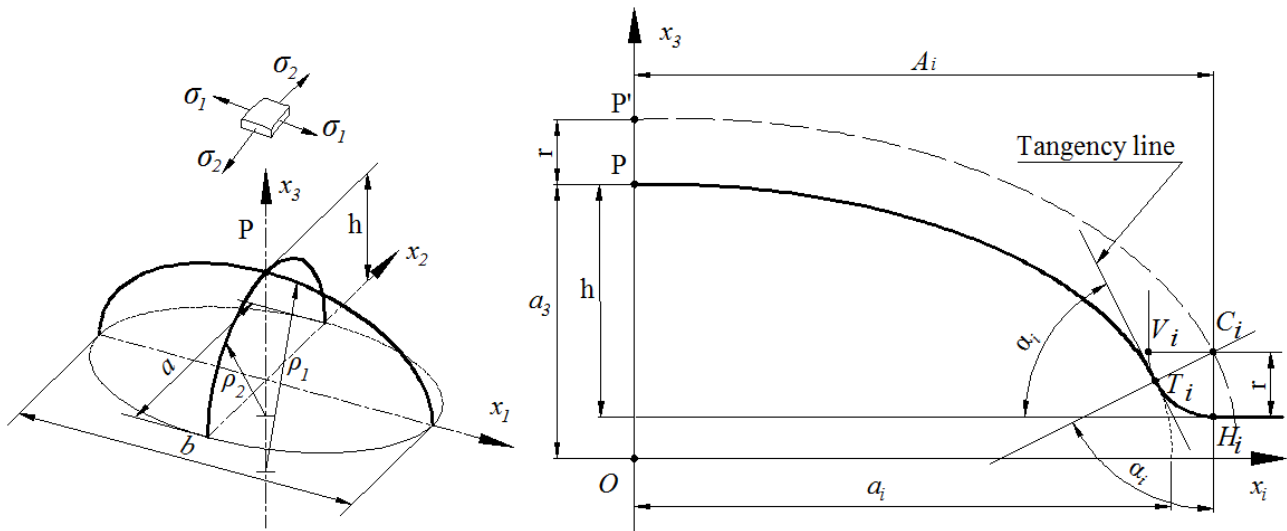


Fig.1. Geometry of the specimen subjected to bulging through a die with elliptical aperture

Principal axes of the ellipsoid. In the geometric schematization adopted by the authors (Fig. 1), A_i ($i=1,2$) and the fillet radius of the die (r) are constant parameters defined by the design of the bulging device, and h is the current value of the polar deflection measured during the experiment. The quantities that must be indirectly determined are the semi-axes of the ellipsoid used to approximate the deformed surface of the specimen: a_i ($i=1, 2, 3$). The curve drawn at an offset distance r from the elliptic arc PT_i ($i = 1,2$) is defined by the following equation:

$$\left(\frac{x_i}{a_i+r}\right)^2 + \left(\frac{x_3}{a_3+r}\right)^2 = 1, (i=1,2). \quad (1)$$

As shown in Figure 1, the points $P'(0, a_3+r)$ and $C_i(A_i, a_3+r-h)$ belong to this offset curve. By consequence, their coordinates must verify Eq. (1):

$$\left(\frac{A_i}{a_i+r}\right)^2 + \left(\frac{a_3+r-h}{a_3+r}\right)^2 = 1, (i=1,2). \quad (2)$$

Eq. (2) leads to the following relationship between the semi-axes a_i ($i=1, 2$):

$$A_1/A_2 = (a_1+r)/(a_2+r) = k \geq 1, \quad (3)$$

($k = A_1/A_2$ is a constant parameter of the bulging device). Due to the fact that the profile of the deformed specimen is assumed to be circular along the minor axis of the die hole, the semi-axes a_2 and a_3 are equal to each other: $a_2=a_3$. Under such circumstances, one may deduce from Eq. (2) written for $i=2$ the following formula that allows the calculation of the minor semi-axes a_2 and a_3 :

$$a_2 = a_3 = \frac{A_2^2 + h^2}{2h} - r. \quad (4)$$

In the next stage, Eqs. (3) and (4) lead to the relationship defining the major semi-axis:

$$a_1 = \frac{A_1}{A_2} \frac{A_2^2 + h^2}{2h} - r. \quad (5)$$

Polar radii of the specimen. When written for $i = 1$, Eq. (1) provides the function describing the profile of the deformed specimen along the major axis of the die hole:

$$x_3 = \sqrt{(a_3 + r)^2 - \left(\frac{a_3 + r}{a_1 + r}\right)^2} x_1. \quad (6)$$

The polar radius of the elliptic arc defined by Eq. (6) can be evaluated as follows:

$$\rho_1 = \frac{(a_1 + r)^2}{a_3 + r} - r. \quad (7)$$

After replacing the semi-axes a_3 and a_1 defined by Eqs. (4) and (5), respectively, Eq. (7) becomes

$$\rho_1 = \left(\frac{A_1}{A_2}\right)^2 \frac{A_2^2 + h}{2h} - r. \quad (8)$$

In the same manner, when written for $i = 2$, Eq. (1) provides the following relationship that defines the other curvature radius at the pole:

$$\rho_2 = a_2 = a_3 = \frac{A_2^2 + h^2}{2h} - r. \quad (9)$$

The angle spanned by the circular profile of the specimen (α_2 - see Figure 1) can be evaluated in the standard manner [5]:

$$\alpha_2 = \arctg \frac{2A_2h}{A_2^2 - h^2}. \quad (10)$$

Polar thickness. In this paper, the polar value of the meridian strain associated to the circular profile of the specimen is evaluated using Kruglov's formula [7]:

$$\varepsilon_2 = \ln(\alpha_2 / \sin \alpha_2). \quad (11)$$

As concerns the other meridian strain (associated to the elliptic profile of the specimen), its calculation is performed by adopting the hypothesis

$$\varepsilon_1 = \beta \varepsilon_2, \quad (12)$$

where

$$\beta = (\rho_2 / \rho_1) \cong \text{const.}, \quad (13)$$

is considered a constant ratio for a given geometry of the die hole. The experimental data plotted on the diagram in Figure 2.b shows only a slight variation of β , thus confirming the validity of the assumption $\beta \cong \text{const.}$ After making use of the law that enforces the volume preservation in connection with Eq. (12), one obtains the following formula for the thickness strain at the pole:

$$\varepsilon_3 = -(\varepsilon_1 + \varepsilon_2) = -(1 + \beta)\varepsilon_2. \quad (14)$$

The current value of the polar thickness can be thus obtained from the relationship

$$t = t_0 e^{-(1+\beta)\varepsilon_2} \quad (15)$$

where t_0 is the initial thickness of the specimen (nominal thickness of the sheet metal).

Equivalent strain and stress. The polar values of the principal stresses are evaluated using Timoshenko's formulas [8]:

$$\sigma_1 = \frac{p\rho_2}{2t} \quad \text{and} \quad \sigma_2 = \frac{p\rho_2}{2t} \left(2 - \frac{\rho_2}{\rho_1}\right) \quad (16)$$

(σ_1 and σ_2 are the meridian and circumferential stresses, respectively). Eqs. (16) lead to the following relationship between σ_1 and σ_2 :

$$\sigma_1 \cong \sigma_2 / (2 - \beta). \quad (17)$$

The significance of the equivalent stress ($\bar{\sigma}$) and equivalent strain ($\bar{\varepsilon}$) can be deduced from the plastic dissipation law:

$$\sigma_1 \dot{\varepsilon}_1 + \sigma_2 \dot{\varepsilon}_2 = \bar{\sigma} \dot{\bar{\varepsilon}}. \quad (18)$$

Eqs. (12) and (13) lead to the approximation $\dot{\varepsilon}_1 = \beta \dot{\varepsilon}_2$. After combining this relationship and Eq. (17) with Eq. (18) one obtains

$$\sigma_2 \dot{\varepsilon}_2 \frac{2}{2 - \beta} = \bar{\sigma} \dot{\bar{\varepsilon}}. \quad (19)$$

In accordance with Eq. (17), the equivalent stress and equivalent strain can be defined as follows:

$$\bar{\varepsilon} = \frac{2}{2 - \beta} \varepsilon_2, \quad \bar{\sigma} = \sigma_2. \quad (20)$$

One may notice that Eqs. (20) reduce to $\bar{\varepsilon} = 2\varepsilon_2$ and $\bar{\sigma} = \sigma_2$ for $\beta = 1$, being thus consistent with the formulas used in the case of the hydraulic bulging through circular dies. Eqs. (16) and (13) provide the following relationship for the equivalent stress:

$$\bar{\sigma} = \sigma_2 = \frac{(2 - \beta)p\rho_2}{2t}. \quad (21)$$

The hardening curve relating the equivalent strain and the equivalent stress can be constructed using Eqs. (20) and (21). These relationships are valid for the hydraulic bulging with dies having both elliptical and circular holes. Eqs. (20) and (21) need the experimental determination of only two process parameters: current value of the pressure acting on the bottom face of the specimen p and the associated polar deflection h .

Experiments

The experiments consisted in hydraulic bulge tests performed on specimens cut from a DC04 steel sheet having the nominal thickness of 0.85 mm. Three ellipticity ratios were used: (a / b): 0.6 (48 / 80); 0.8 (64 / 80), and 1 (circular hole with a diameter of 80 mm). The fillet radius of the die was $r = 4$ mm in all cases. The current values of the pressure and polar height were continuously recorded using an ARAMIS system. The estimations of the polar radius provided by the ARAMIS system for different stages of the bulging process were used for comparison with the values of the radius ρ_2 obtained from Eq. (9). The circumferential strains measured by the ARAMIS system along the minor axis of the die hole were also replaced in Eq. (20) for obtaining different points of the curve equivalent stress – equivalent strain.

Results

Bulge radius and polar height. Figure 2 shows the evolution of the polar radius ρ_2 as a function of the polar deflection h , for different values of the ellipticity ratio. One may notice that the results obtained using the analytical formulas deduced in this paper are in good agreement with the experimental data provided by the ARAMIS system. Figure 3 presents the evolution of the curvature ratio β as a function of the polar deflection h , for different values of the ellipticity ratio. As one may expect, the closer to one is the ellipticity ratio a / b, the more stable is β . Figure 3 shows a slight decrease of the curvature parameter β only in the case of the strongest ellipticity (a / b = 0.6). For larger ratios a / b, the variation of the curvature parameter β is insignificant.

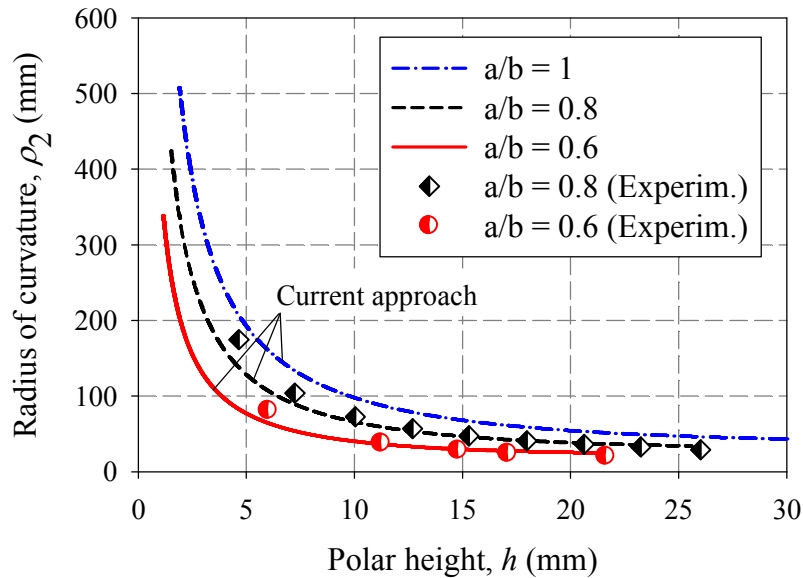


Fig. 2. Curvature radius vs. polar height

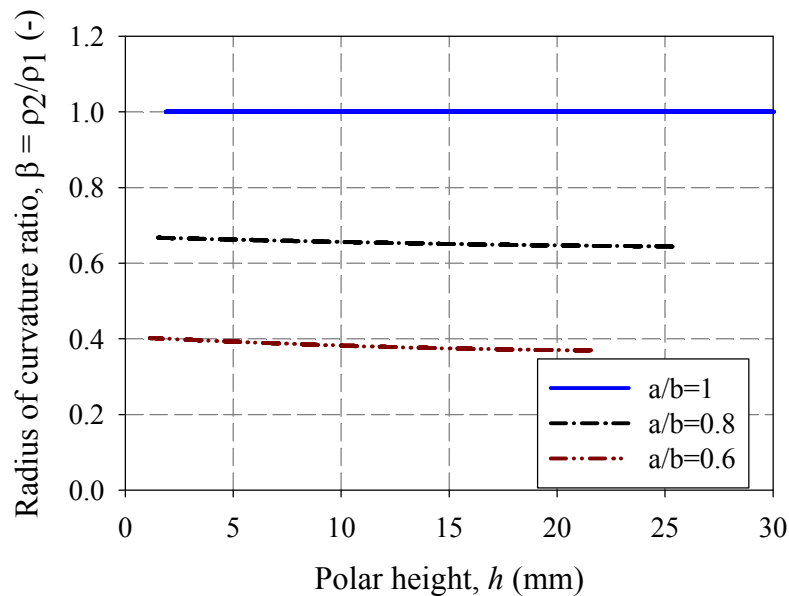


Fig. 3. Curvature ratio vs. polar height

Equivalent stress – equivalent strain curves. Figure 4 shows the curves equivalent stress – equivalent strain obtained using the methodology proposed by the authors. Some discrete points resulted from measurements performed with the ARAMIS system have been also plotted on the diagram. These points have been determined by coupling different values of the circumferential strain ε_2 (ARAMIS measurement) with the equivalent stress $\bar{\sigma}$ resulted from Eq. (21) after replacing the curvature radius ρ_2 also provided by the ARAMIS system. Figure 4 reveals a good agreement between the curves drawn using the new methodology and the experimental points.

Conclusion

This paper describes a new procedure for the experimental determination of the curves relating the equivalent stress and the equivalent strain by means of hydraulic bulge tests with elliptical dies. The main advantage of the methodology proposed by the authors consists in the fact that only two

process parameters should be recorded during the experiment (pressure acting on the bottom surface of the specimen and polar deflection). The results obtained using the new procedure for ellipticity ratios of 0.8 and 0.6 are in good agreement with experimental data measured with an ARAMIS system.

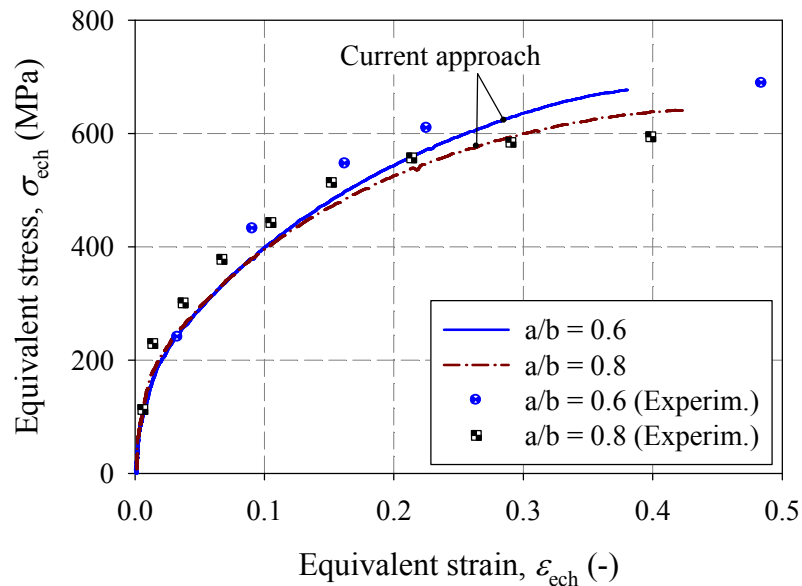


Fig. 4. Equivalent stress - equivalent strain curves

Acknowledgements

This paper was supported by the projects: "Development and support of multidisciplinary postdoctoral programmes in major technical areas of national strategy of Research - Development - Innovation" 4D-POSTDOC, contract no. POSDRU/89/1.5/S/52603, POSDRU/107/1.5/S/78534 and PCCE 100/2010.

References

- [1] M.I. Yousif, J. L. Duncan and W. Johnson, Plastic deformation and failure of thin elliptical diaphragms, *Int. J. Mech. Sci.* 12 (1970) 959-972.
- [2] D. Banabic, T. Bălan and D.S. Comşa, Closed-form solution for bulging through elliptical dies, *J. Mater. Process. Tech.* 115 (2001) 83-86.
- [3] A.R. Ragab, O.E. Habib, Determination of the equivalent stress versus equivalent strain rate behaviour of superplastic alloys in biaxial stress systems, *Mater. Sci. Eng.* 64 (1984) 5-14.
- [4] D.W.A Rees, Plastic flow in the elliptical bulge test, *Int. J. Mech. Sci.* 37 (1995) 373-389.
- [5] L. Lăzărescu, D.S. Comşa, D. Banabic, Analytical and experimental evaluation of the stress-strain curves of sheet metals by hydraulic bulge tests, *Key Eng. Mat.* 473 (2011) 352-359.
- [6] L. Lăzărescu, D.S. Comşa, D. Banabic, Determination of stress-strain curves of sheet metals by hydraulic bulge test, *AIP Conf. Proc.* 1353 (2011) 1429-1434.
- [7] A.A. Kruglov, F.U. Enikeev and R.Y. Lutfullin, Superplastic forming of a spherical shell out a welded envelope, *Mat. Sci. Eng.* A323 (2002) 416-426.
- [8] S. P. Timoshenko, S. W. Krieger, *Theory of plates and shells*, McGraw-Hill, 1959.

Material Forming ESAFORM 2012

10.4028/www.scientific.net/KEM.504-506

A Procedure for the Evaluation of Flow Stress of Sheet Metal by Hydraulic Bulge Test Using Elliptical Dies

10.4028/www.scientific.net/KEM.504-506.107